Nano/micro hybrid scaffold of PCL or P3HB nanofibers combined with silk fibroin for tendon and ligament tissue engineering

Elham Naghashzargar[1,2], Silvia Farè[2,3], Valentina Catto[2,3], Serena Bertoldi[2,3], Dariush Semnani[1], Saeed Karbasi[4], Maria Cristina Tanzi[2,3]

[1] Department of Textile Engineering, Isfahan University of Technology, Isfahan - Iran
[2] BioMatLab, Department of Chemistry, Materials and Chemical Engineering G. Natta, Politecnico di Milano, Milan - Italy
[3] Local Unit Politecnico di Milano, INSTM, Milan - Italy
[4] Department of Medical Physics and Biomedical Engineering, School of Medicine, Isfahan University of Medical Sciences, Isfahan - Iran

ABSTRACT

A novel biodegradable nano/micro hybrid structure was obtained by electrospinning P3HB or PCL nanofibers onto a twisted silk fibroin (SF) structure, with the aim of fabricating a suitable scaffold for tendon and ligament tissue engineering. The electrospinning (ES) processing parameters for P3HB and PCL were optimized on 2D samples, and applied to produce two different nano/micro hybrid constructs (SF/ES-PCL and SF/ES-P3HB).

Morphological, chemico-physical and mechanical properties of the novel hybrid scaffolds were evaluated by SEM, ATR FT-IR, DSC, tensile and thermodynamic mechanical tests. The results demonstrated that the nanofibers were tightly wrapped around the silk filaments, and the crystallinity of the SF twisted yarns was not influenced by the presence of the electrospun polymers. The slightly higher mechanical properties of the hybrid constructs confirmed an increase of internal forces due to the interaction between nano and micro components. Cell culture tests with L929 fibroblasts, in the presence of the sample eluates or in direct contact with the hybrid structures, showed no cytotoxic effects and a good level of cytocompatibility of the nano/micro hybrid structures in term of cell viability, particularly at day 1. Cell viability onto the nano/micro hybrid structures decreased from the first to the third day of culture when compared with the control culture plastic, but appeared to be higher when compared with the uncoated SF yarns. Although additional in vitro and in vivo tests are needed, the original fabrication method here described appears promising for scaffolds suitable for tendon and ligament tissue engineering.

Key words: Electrospinning, Hybrid scaffolds, L929 fibroblasts, Polycaprolactone, Poly(3-hydroxybutyrate), Silk fibroin, Tendon and ligament

Accepted: June 11, 2014

INTRODUCTION

The dense connective tissues of tendons and ligaments, mainly composed of collagen type I, generate movement and stability of tissues in the human body (1). Ruptures and tearing can cause great pain and instability, impairing the functionality of the joint complex. These tissues have a low healing potential and limited vascularization, so that sutures are an ineffective repair procedure, unable to restore the preinjury properties of the tissue (2). The anterior cruciate ligament (ACL) is the most commonly injured ligament of the knee, with an annual incidence rate between 100,000 and 200,000 in the United States (3). Current surgical approaches in ACL repair consist of reconstruction with autograft or allograft. Although the use of autografts is successful, there is the drawback of requiring harvesting of normal uninjured tissue from another part of the patient knee, with donor site morbidity and pain. The use of allografts can alleviate most of the issues associated with the donor site in autologous grafts. However, contemporary studies have suggested a relatively high rerupture rate associated with allografts, particularly in younger, more active patients (4). Because of the inadequacy of biological grafts, there has been interest in developing synthetic ACL substitutes since the early 1970s (5-7). Although these grafts have had sufficient initial tensile strength, all

showed similar problems due to particulate debris in the knee causing particulate-induced synovitis and, ultimately, graft failure (8). The US Food and Drug Administration (FDA) removed all synthetic ACL grafts from the market, and currently no synthetic replacements for primary ACL reconstruction are unconditionally approved for medical use in the United States. Some of these synthetic grafts were conditionally approved by the FDA only for revision surgeries (1).

Recently, tissue engineering has emerged as a promising approach for the regeneration of damaged ligaments, with similar mechanical and biochemical properties (9, 10). The scaffold, influencing cell activity and extracellular matrix (ECM) formation, is a key component for ligament tissue engineering. Both in vivo and in vitro systems can be used for the development of a functional engineered ligament. In vivo ligament engineering uses a scaffold that is designed to be implanted into the host and encourage tissue ingrowth and neoligament formation: this scaffold may be seeded with cells, or modified to enhance biocompatibility and host cellular response. Conversely, in vitro systems use a bioreactor in which the ligament is developed on a structural scaffold for subsequent host implantation. The potential tissue replacement rendered by this system would allow immediate implantation of a functional ligament that is expected to undergo physiological remodeling in the host knee. The successful implementation of either system requires that the cells that populate the scaffold lay down collagen in an organized fashion similar to the native ligament, and that this neoligament holds the mechanical and biochemical properties required for physiologic loading following implantation (7, 11). Therefore, one of the major goals of tendon and ligament tissue engineering is to design a proper biodegradable scaffold that matches the mechanical (tensile strength, viscoelastic and fatigue properties) and biochemical properties of native tissues (12).

Several research groups have reported on collagen (13), biodegradable synthetic polymers (14, 15) and composite materials (16) to fabricate potential ACL scaffolds. Collagen has been extensively investigated, but despite the different methods used to improve its mechanical properties, the strength of the collagen scaffolds is still lower than desired. Hence, other biologic materials, such as hyaluronic acid (17), chitosan (18) and alginate (19), were investigated in ligament tissue engineering.

In recent years, silk fibroin (SF) has been increasingly investigated as a possible scaffold for ligament tissue reconstruction due to its biocompatibility, slow degradability and remarkable mechanical properties (20-24). Silk fibers provide an excellent combination of lightweight (1.3 g/cm^3), high strength (up to 4.8 GPa), and remarkable deformation (up to 35%) (25).

Various methods have been tried to model the mechanical behavior of tendon and ligaments scaffolds. Because of the mechanical properties similar to textile structures, such as the viscoelastic and nonlinear behavior, many fabrication textile techniques have been developed to design different scaffolds (26). In particular, textile-based scaffolds like braided (27), woven (28), wire-rope (29) or knitted (30) structures have been widely used in the last decade.

Architecture is an important parameter to be considered in the scaffold design because it can modulate the biological response and the long-term clinical success of the scaffold. The scaffolds can vary in terms of morphology (pore diameter, porosity, surface area), and mechanical properties under tensile and cyclic loading, according to fabrication parameters such as materials selection, fiber diameter, braiding and twisting angles and yarn density (31).

Different cell types have been selected for seeding into polymeric scaffolds to regenerate damaged tendon/ligament tissues. The most commonly used are fibroblasts, tenocytes and mesenchymal stem cells/marrow stromal cells (MSCs) (32), which can be responsible for secreting and maintaining the ECM. Fibroblasts are the predominant cell type (33), although MSCs proliferate quickly and produce more collagen in comparison with fibroblasts. These cells have demonstrated good capability of regenerating ligament/tendon tissues in in vitro and in vivo tests (2).

Attempts to improve cell adhesiveness and colonization of the scaffolds using a gel system, such as fibrin or collagen gel to support cell seeding, have demonstrated instability in a dynamic environment such as the knee joint (34) and problems in nutrient transmission (28).

The major component of natural ECM of ligaments and tendons is collagen I, with a fibrous structure made of fiber bundles varying in diameter from 50 to 500 nm. To mimic the nano scale architecture, a few technologies of electrospinning (35), salt leaching (36) and self assembly (37) have been used to fabricate nanofiber scaffolds with different biodegradable polymers (38).

Nanofibrous scaffolds have a high surface to volume ratio. This enhances cell adhesion that leads to increased cell migration, proliferation and differentiated functions (38). However, a nanofibrous matrix alone would not be sufficiently strong for engineering a fibrous connective tissue such as that of tendons and ligaments (39).

Among the various textile and fiber-based scaffolds (9), hybrid structures comprising both microfibers and nanofibers have been developed to derive mechanical integrity from the microfibers, and a large favorable surface for cell attachment and growth from the nanofibers. Also, hybrid structured scaffolds composed of a textile structure and electrospun nanofibers have been recently investigated (28).

Surface modifications by coating with nanofibers can be particularly effective in aiding cell attachment, growth, proliferation, and ECM deposition. Electrospun polymer nanofibers possess a high surface area to volume ratio. Through the process of electrospinning, fibers with diameters ranging from a few nanometers to millimeters

can be obtained. This will allow for increased cell adhesion, suggesting that the morphology of the underlying scaffold may affect ECM production. Synthetic biodegradable polymers – e.g., polylactic glycolic acid (PLGA), polycaprolactone (PCL) (40, 41) – and natural polymers – e.g., collagen, fibroin, poly(3-hydroxybutyrate) (P3HB) (42) – have been widely investigated to produce electrospun nanofibers.

A scaffold composed of a PLGA knitted structure coated by PLGA nanofibers demonstrated good cell viability and proliferation (39). Besides, an SF-knitted structure coated with bFGF-releasing ultrafine bioactive PLGA fibers enhanced collagen production and resulted in a stronger construct in ligament and tendon tissue engineering (2).

Zhou et al (43) proposed a method of producing the hybrid yarn by depositing poly(ethylene oxide) (PEO) nanofibers onto polyamide (PA) filaments and using a twisting process to improve cohesion between nano and micro components. These authors expected these hybrid structures to be particularly promising for improving the performance of scaffolds in tendon and ligament tissue engineering when using suitable biopolymers.

In our approach, a novel biodegradable nano/micro hybrid scaffold was developed by electrospinning P3HB or PCL nanofibers onto a twisted silk structure to design a suitable scaffold for tendon and ligament tissue engineering. PCL was chosen as one of the most commonly used biodegradable polymers due to its lack of toxicity, low cost and slow degradation rate, which are necessary for this specific application (44). On the other hand, the potential application of P3HB in tendon and ligament tissue engineering was pointed out for the first time by Rathbone et al (45). P3HB is one of the well-characterized homopolymers of the polyhydoxyalkanoate family which have demonstrated good biocompatibility and biodegradability (46). Previous studies of P3HB have demonstrated good L929 cell adhesion, excellent biocompatibility and lack of toxicity (45).

In this work, the electrospinning processing parameters for P3HB and PCL were optimized. Then, a twisted SF structure was coated by electrospun P3HB or PCL nanofibers. Morphological, chemicophysical and mechanical properties of this novel scaffold were investigated. To investigate possible cytotoxic effects and cytocompatibility properties of this hybrid scaffold, a preliminary in vitro cell study was carried out with L929 cells.

MATERIALS AND METHOD

Materials

All basic chemical materials were obtained from Sigma-Aldrich unless specified otherwise. P3HB was kindly supplied by the TianAn Biopolymer Company (China). SF yarns were purchased from Kiashahr Co. (Iran). Raw silk

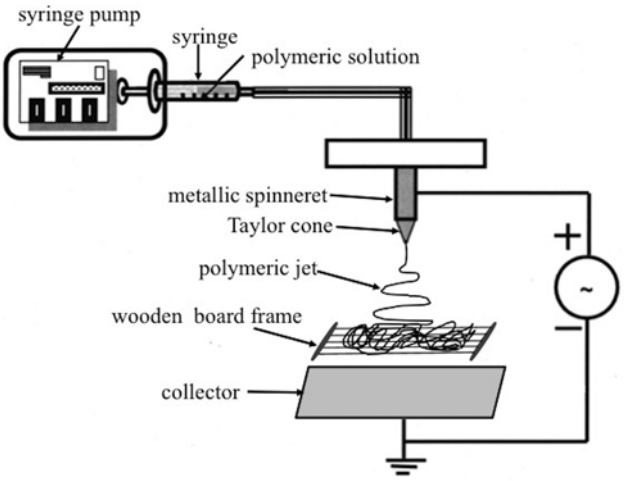

Fig. 1 - *Home-made electrospinning apparatus for the fabrication of the nano/micro hybrid scaffold.*

yarns consisted of four twisted filaments, each of them with 64 filaments; therefore, the total number of filaments in each yarn was equal to 256 (linear density of approximately 200 Den).

According to previous investigations (2, 29), the raw silk yarns were boiled in a degumming solution of 0.25% Na_2CO_3 solution at 95°C-98°C for 30 minutes. The process was repeated with fresh degumming solution for 60 minutes, followed by rinsing with distilled water. The parameters used for the degumming process ensured the complete removal of sericin, as demonstrated by the color change (white from yellow) of the silk yarns, according to the literature (22, 47). SF yarns were immersed in methanol overnight to clean the silk yarns and dried for 24 hours before the fabrication of the nano/micro hybrid scaffolds.

Electrospinning of P3HB and PCL

PCL (M_n=80,000) and P3HB (M_w=500,000) were separately dissolved in dimethylformamide (DMF) and chloroform ($CHCl_3$) in a 1:9 ratio at room temperature and at 65°C, respectively. Nanofibrous mats were produced with a home-made vertical electrospinning apparatus using a flat collector (Fig. 1). Each polymeric solution was placed in a 20-mL glass syringe and forced by a syringe-pump (KDS 100; KD Scientific) into the spinneret, a stainless steel capillary tube (inner diameter = 1.1 mm). The spinneret was connected to the positive output of a high voltage power supply (HCN 35-12500; Fug Elektronik GmbH), and the negative pole was joined to the fiber collector, a metallic plate covered with aluminum foil.

Different combinations of electrospinning parameters, as shown in Table I, were explored to investigate the optimal experimental set-up related to dimension and uniformity of the fibers in the electrospun PCL (ES-PCL) and

TABLE I - PROCESSING PARAMETERS FOR PCL AND P3HB ELECTROSPINNING

	Test no.	Concentration (% w/v)	Voltage (kV)	Solution flow rate (ml/hour)	Distance from spinneret to collector (cm)
PCL	A1	20	24	0.4	18
	B1	20	16	0.3	16
	C1	20	24	0.5	20
	D1	17	24	0.4	18
P3HB	A2	5	20	0.5	20
	B2	5	24	1	20
	C2	5	24	0.5	20
	D2	5	24	1	22

PCL = polycaprolactone; P3HB = poly(3-hydroxybutyrate).

P3HB (ES-P3HB) mats. For the complete evaporation of the solvents, ES-PCL and ES-P3HB mats were placed under a fume hood at room temperature overnight.

Fabrication of nano-micro hybrid scaffolds

Nano/micro hybrid scaffolds were fabricated by electrospinning of PCL or P3HB onto the surfaces of parallel SF yarns, followed by the twisting of nanofiber-coated SF yarns. Specifically, 5 unidirectionally aligned SF yarns (length = 25 cm) were fixed with 5-mm spacing on a wooden structure and placed above the flat collector to allow PCL or P3HB electrospun fiber deposition onto the SF yarns, as shown schematically in Figure 1. The deposition time and distance between the wooden structure and the flat collector were optimized. The nanofiber-coated SF yarns were then twisted by a hand-twisting process to fabricate the nano/micro hybrid scaffolds. As previously reported (29), the twisted yarns were relaxed in the oven at 50°C for 30 minutes. The temperature of the treatment was adjusted from 100°C (29) to 50°C due to PCL and P3HB thermal transition temperatures.

Scanning electron microscopy

ES-PCL and ES-P3HB mats and nano/micro hybrid scaffolds were observed by scanning electron microscopy (SEM, Cambridge Instrument Stereoscan 360). Specimens were mounted onto aluminum stubs, sputter-coated with gold (Edwards Sputter Coater 5150B), and observed at different magnification (×15 to ×2,000) at an accelerating voltage of 10 kV. SEM images were elaborated using ImageJ software (US National Institute of Health, Bethesda, MD, USA), and the average nanofiber diameter was calculated by measuring 30 fibers for each sample.

Tensile mechanical tests

Tensile properties of the nano/micro hybrid structures were investigated by a MTS testing machine (MTS System, model 1M/H). Mechanical tests were performed on dry specimens (gauge length = 20 mm, n=5) of twisted SF yarns, SF/ES-PCL and SF/ES-P3HB samples. Tensile tests were carried out at a crosshead speed of 50 mm/minute (preload = 1 N) until specimen failure. The load (N) and extension (mm) were recorded; the failure load (L_{max}) and extension (e_{max}) were determined after plotting load/extension curves (22).

Dynamic mechanical analysis

Dynamic mechanical analysis (DMA) was performed using a DMA analyzer (Q800, TA Instrument) in tensile mode in the temperature range 35°C-90°C, with a heating rate of 3°C/minute, 1 Hz and 15 μm strain application. Storage modulus (E′), loss modulus (E′′) and Tan delta (Tanδ = E′′/E′) were recorded. The tests were performed in duplicate, according to the Standard Test Method for Assignment of the Glass Transition Temperature By Dynamic Mechanical Analysis (ASTM 1640-99), using SF, SF/ES-PCL or SF/ES-P3HB specimens (length = 20 mm, n=2).

Chemicophysical characterization

Possible interactions between SF yarns and ES-PCL or ES-P3HB were investigated by Fourier transform infrared (FTIR) spectroscopy with a Thermo Nicolet 6700 FT-IR spectrometer equipped with an attenuated total reflectance (ATR; Single Bounce) accessory and ZnSe crystal.

Differential scanning calorimetry (DSC) analyses were performed on approximately 5 mg of SF yarns, ES-PCL, ES-P3HB, SF/ES-PCL and SF/ES-P3HB with a Q200 DSC (TA Instruments) using standard aluminum pans. Specimens were heated from 20°C up to 500°C, under N_2 atmosphere, at a 10°C/minute scanning rate. Specifically, the melting/decomposition peak values were assessed and calculated from the DSC thermograms.

In vitro cytocompatibility

Cytotoxicity of the extracts and cytocompatibility of SF yarns, SF/ES-PCL and SF/ES-P3HB were assessed using an L929 murine fibroblasts cell line (ECACC No. 85011425).

Cytotoxicity tests

Extracts were obtained according to UNI EN ISO 10999-5. Specimens were in 70% (v/v) ethanol aqueous solution, air-dried overnight, and then rinsed in sterile

phosphate-buffered saline (PBS). Three samples for each material were immersed in 1 ml Dulbecco's modified Eagle's medium (DMEM) with 10% fetal bovine serum (FBS) and 1% penicillin/streptomycin, maintaining a ratio material/medium of 0.1 g/mL. After 1, 3 and 7 days of incubation, medium extracts were put in contact with L929 (cell density = $1x10^4$ cells/mL) in 96-well tissue culture polystyrene (TCPS) plate for 24 hours. Tests were performed in triplicate. Cell viability was evaluated by 3-(4,5-dimethylthiazol-2-yl)-2,5-diphenyltetrazolium bromide (MTT) biochemical assay (M5655; Sigma). Culture medium was replaced with 200 µL of MTT solution and incubated for 4 hours at 37°C and 5% CO_2. Afterwards, MTT solution was replaced with 200 µL of dimethyl sulfoxide (DMSO; Merk), and the multiwell plate was shaken until complete salt crystal dissolution. Absorbance was measured using a Tecan Genius Plus plate reader (test wavelength: 570 nm; reference wavelength: 630 nm). Measured absorbance was expressed as relative ratio over control cells on TCPS in DMEM incubated for 1, 3 and 7 days.

Cytocompatibility tests

For direct seeding, SF, SF/ES-PCL and SF/ES-P3HB samples were disinfected by soaking in 70% (v/v) ethanol aqueous solution, air-dried overnight, and then rinsed in sterile PBS before L929 cell seeding (cell density = $1x10^5$ cells/mL). After 24 hours and 3 days of incubation, cell viability was assessed using MTT colorimetric assay, as previously described.

Statistical analysis

Data for electrospun nanofiber size and tensile tests were statistically compared with Student's *t*-test and 1-way ANOVA, using SPSS 13.0 software; the significance level was set at 0.05. Finally, to compare data between groups, analysis of variance was performed by post hoc Scheffé test. The normality of all data was checked before each statistical comparison.

RESULTS AND DISCUSSION

Morphology of electrospun PCL and P3HB nanofibers

The mean values and standard deviation (SD) of the nanofiber diameters for PCL and P3HB electrospun mats, as measured by SEM analysis by ImageJ software, are reported in Table II.

According to ANOVA, there was a significant difference ($P<0.05$) between the average diameter values of PCL or P3HB nanofibers obtained in the electrospinning conditions considered (see Tab. I for the respective processing parameters). All samples of P3HB nanofibers were statistically different according to Scheffé test. The processing parameters of the A2 test were recognized as the best ones due to the smallest diameter and standard deviation values in comparison with the other conditions. In the case of PCL, the electrospinning parameters of the A1 test were chosen due to the lower dispersion of diameter values. Therefore, the concentration, voltage, distance of spinneret to collector and solution flow rate conditions were optimized as 20%, 12 kV, 18 cm and 0.4 ml/hour for PCL, and 5%, 10 kV, 20 cm and 0.5 ml/hour for P3HB, respectively. Figure 2 shows SEM images of PCL and P3HB nanofiber samples obtained in the different electrospinning test conditions, together with the respective histograms for diameter distributions.

TABLE II - DIAMETERS OF PCL AND P3HB NANOFIBERS AFTER DIFFERENT ELECTROSPINNING CONDITIONS DESCRIBED IN TABLE I

	Test no.	Average (micron)	SD (micron)
PCL	A1	1.906	0.350
	B1	1.363	0.538
	C1	1.774	0.523
	D1	1.980	0.261
P3HB	A2	1.271	0.230
	B2	1.663	0.486
	C2	1.297	0.435
	D2	1.736	0.500

Values are means and standard deviation (SD).
PCL = polycaprolactone; P3HB = poly(3-hydroxybutyrate).

In the previous works, PLGA nanofibers were produced in the range of 300-900 nm diameter size for tendon and ligament hybrid scaffolds (13-15, 20-22, 25). Also, the average diameters of electrospun P3HB and PCL were reported to be 993 nm (15) and 431 nm (28), respectively. The size of nanofibers fabricated in the present work was similar for P3HB and slightly higher for PCL, but these can reasonably be considered acceptable for tendon and ligament hybrid scaffolds.

Morphology of the nano/micro hybrid scaffold

Once optimized the electrospinning conditions, SF/ES-PCL and SF/ES-P3HB hybrid scaffolds were fabricated, following the procedure described below.

The 2 main variable parameters – namely, coating distance and coating time – were set up for the electrospinning process. The coating distance determines the relative position of SF yarns to the needle and is therefore most likely to influence the coating density and length along the filaments (47). In this way, the optimal coating positions were found to be 14 and 16 cm for

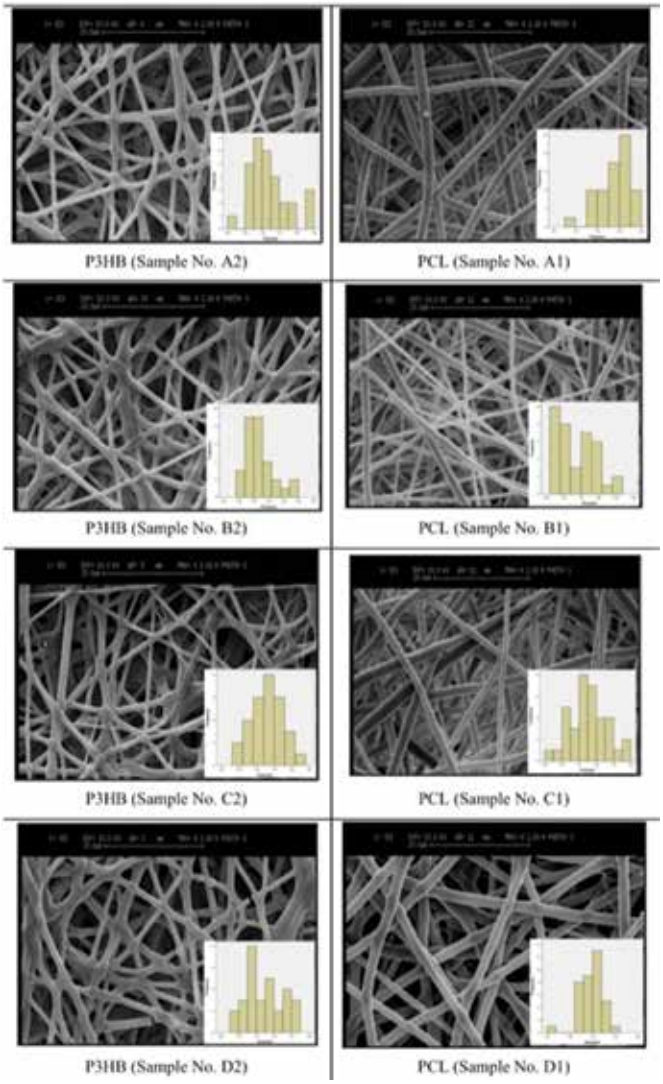

Fig. 2 - *SEM images of PCL and P3HB nanofibers samples obtained in the different electrospinning test conditions described in Table I. Insert boxes: related histograms of diameter distributions. PCL = polycaprolactone; P3HB = poly(3-hydroxybutyrate).*

PCL and P3HB, respectively, a distance at which that the nanofibers could easily be gathered on the surface of the SF yarns.

To find the best coating morphology, the coating time was changed, while other electrospinning parameters were kept constant. For this reason, SF yarns were coated for different periods of time – namely, 5, 15 and 25 minutes. Figure 3 shows representative SEM micrographs of samples of SF parallel yarns coated by P3HB electrospun nanofibers, and twisted after each coating time. By increasing the coating time, the nanofibers became tightly wrapped around the silk filaments and the SF yarn surface was completely covered by nanofibers after 25 minutes. The morphology of SF/ES-PCL samples was very similar to that of SF/ES-P3HB (images not shown).

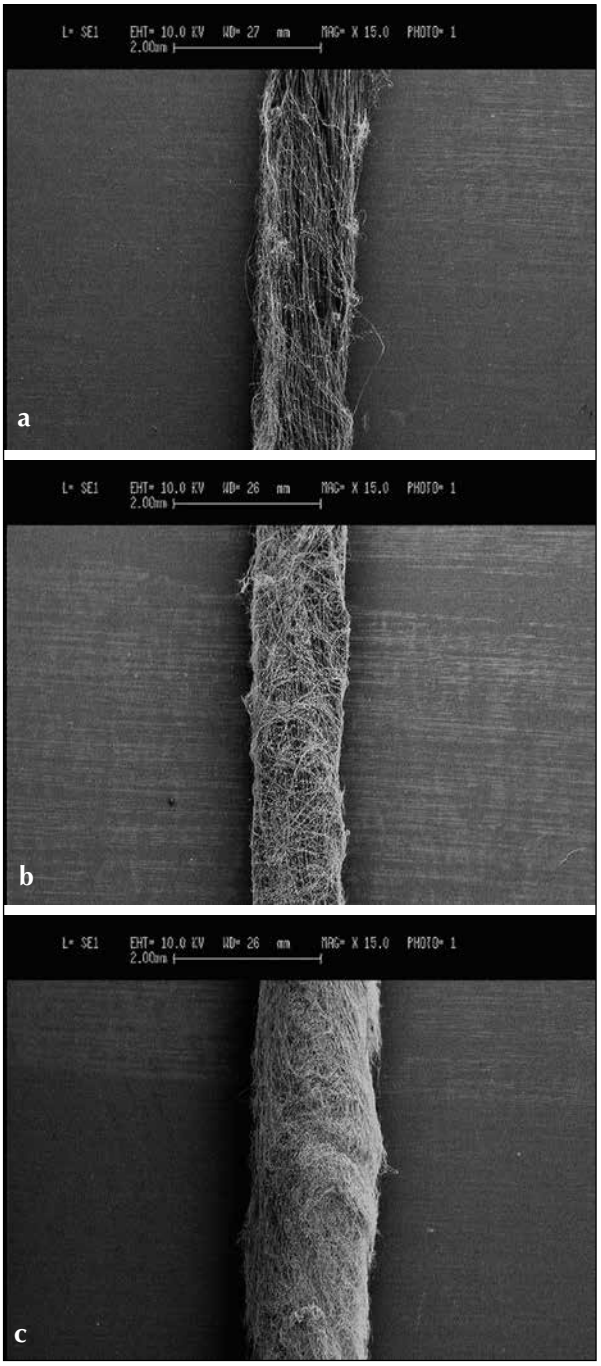

Fig. 3 - *The effect of the electrospinning coating time on nano/micro hybrid scaffolds of silk/ES-P3HB in 5 minutes **(a)**, 15 minutes **(b)** and 25 minutes **(c)**. Scale bar: 2 mm. ES = electrospun; P3HB = poly(3-hydroxybutyrate).*

Uniaxial tensile mechanical tests

Representative load-displacement curves obtained for uniaxial tensile tests performed on SF/ES-PCL and SF/ES-P3HB samples and twisted SF yarns (SF, as control samples), are reported in Figure 4. The first part of the curve represents the toe region, with a relatively low slope (i.e.,

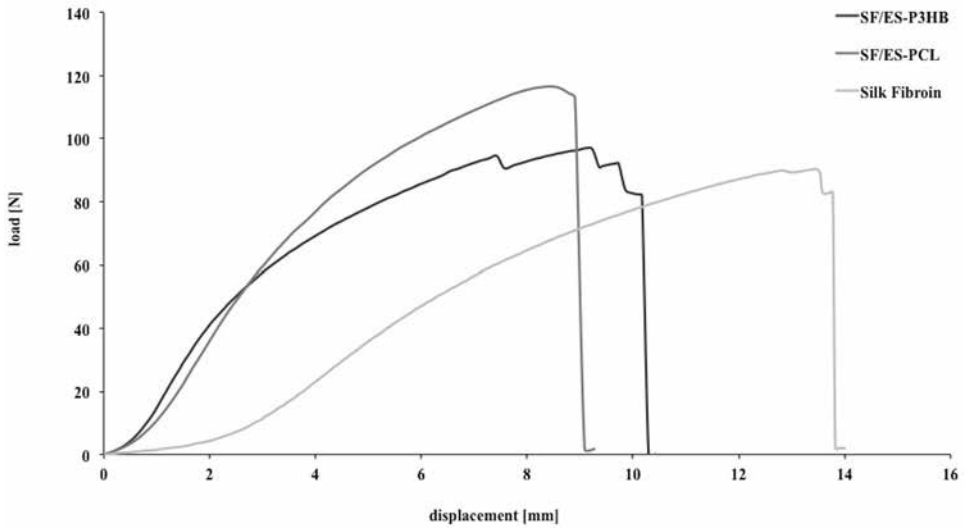

Fig. 4 - *Representative load-displacement curves for twisted SF yarns, SF/ES-PCL and SF/ES-P3HB hybrid structures. ES = electrospun; PCL = polycaprolactone; P3HB = poly(3-hydroxybutyrate); SF = silk fibroin.*

low stiffness), corresponding to the uncrimping of crimp in SF yarns. As it is possible to observe in Figure 4, the toe region for the SF sample reached a higher displacement (Δl=3 mm) than SF coated with electrospun PCL or P3HB (Δl<1 mm). By using PCL or P3HB nanofibers as a coating in nano/micro hybrid yarns, the stiffness in the toe region of the respective curves (i.e., the load necessary to stretch out the crimp of the SF yarns) was higher than that of the SF twisted yarns. This is possibly caused by an increase of the cohesion between the nano (ES-PCL or ES-P3HB) and the micro (SF yarns) parts of the structure. As the yarns become uncrimped, the twisted structures are stretched, showing a stiffer behavior (i.e., linear region). In addition, in the linear region, the SF/ES-coated hybrid structures exhibited a higher slope than the SF twisted structure. Subsequently, when individual fibrils within the structure began to fail, damage accumulated and the structure started to fail (i.e., failure region) (22).

Maximum load and extension values for twisted SF yarns, SF/ES-PCL and SF/ES-P3HB scaffolds, calculated by SPSS software, are reported in Table III.

According to data reported in Table III, the SF/ES-PCL sample exhibited the maximum L_{max} value, but the least e_{max}. By contrast, the SF control structure demonstrated the least maximum load but the higher extension value. The mechanical parameters considered for SF/ES-P3HB were in the range of the values obtained for twisted SF and SF/ES-PCL. This means that the presence of electrospun nanofibers in the nano/micro hybrid yarns led to a decrease of the extension ($P<0.05$) and an increase of the maximum load ($P<0.05$). According to the Scheffé test, the difference between SF/ES-PCL and SF/ES-P3HB samples was not significant ($P>0.05$).

The higher L_{max} value for the nano/micro hybrid structures confirmed an increase of internal forces due to the interaction between nano and micro components. In addition, the hybrid structures mainly derive their mechanical properties from the twisted SF yarns, but nanofibers lock up the structure components, leading to a reduced e_{max} value. The fact that coating by electrospinning can improve the mechanical properties of the final structure in hybrid scaffolds was pointed out by Sahoo et al (28).

Finally, by changing the number of twisted SF yarns in the hybrid structure and selecting the appropriate one relative to individual native tissues, the mechanical properties of the final structure can be adapted to different natural tendon and ligament tissues properties. Therefore, by coating the SF yarns with electrospun nanofibers, the mechanical properties can be made more similar to those of native tissues (29).

TABLE III - MAXIMUM LOAD AND EXTENSION OF TWISTED SF YARNS, SF/ES-PCL AND SF/ES-P3HB HYBRID STRUCTURES

	SF	SF/ES-P3HB	SF/ES-PCL
Maximum load, L_{max} (N)	92.6±8.2	97.6±11.4	110.5±6.6
Maximum extension, e_{max} (mm)	11.5±1.6	9.8±1.4	7.9±1.8

Values are means ± SD, n=5.
ES = electrospun; PCL = polycaprolactone; P3HB = poly(3-hydroxybutyrate); SF = silk fibroin.

Dynamic mechanical analysis

In the temperature range considered, no thermal transitions were detected by observing the storage modulus (E'; Fig. 5a) and the Tanδ (Fig. 5b) behavior of all scaffolds. In fact, SF showed endothermic transitions at higher temperatures (180°C and 215°C), related to thermal motions and/or melting phenomena involving amorphous SF chain

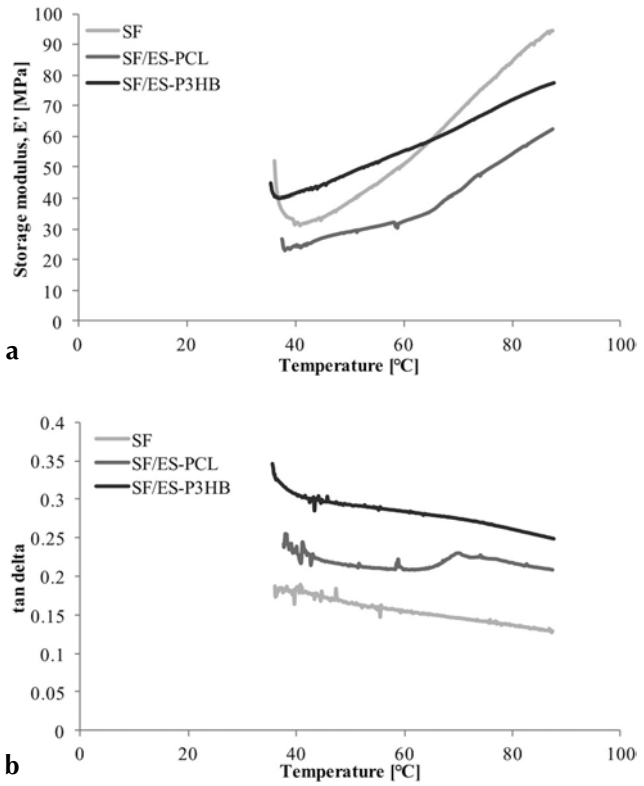

Fig. 5 - *Thermomechanical analysis of twisted silk fibroin (SF), SF/ES-P3HB and SF/ES-PCL as a function of temperature:* ***a)*** *storage modulus (E');* ***b)*** *Tan delta. ES = electrospun; PCL = polycaprolactone; P3HB = poly(3-hydroxybutyrate).*

segments. The increase of E' beyond 60°C is probably due to an increase of SF yarn stiffness by increasing the test temperature. The Tanδ values did not show any differences among SF and PCL and PH3B coated SF structures, showing that the higher elastic contribution and the viscous contribution of SF to the mechanical behavior of the hybrid scaffolds were not influenced by the test temperature. In addition, the coating with ES-PCL or ES-P3HB did not change the viscoelastic behavior of the twisted SF structure.

Thermal properties analysis

The thermal transitions of the base materials (SF yarns, ES-PCL and ES-P3HB) and the 2 nano/micro hybrid structures (SF/ES-PCL and SF/ES-P3HB) were investigated by DSC analysis. The endothermic peak temperature and related enthalpy values, as derived from the DSC patterns analysis, are reported in Table IV.

SF yarns displayed a broad endotherm peak at high temperature, attributed to the thermal decomposition of a well-organized crystalline SF structure (48). ES-PCL showed an endothermic transition related to the melting temperature, with a low enthalpy value, of the PCL

TABLE IV - MELTING TEMPERATURES (T_m) AND VARIATIONS OF ENTHALPY (ΔH) OF SF YARNS, ES-PCL AND ES-P3HB, AND OF NANO/MICRO HYBRID STRUCTURES (SF/ES-PCL AND SF/ES-P3HB)

	T (°C)	ΔH (J/g)
SF	315.4	292.3
ES-PCL	58.2	64.1
ES-P3HB	176.5	69.4
	281.6	512.6
SF/ES-PCL	315.3	288.0
SF/ES-P3HB	318.2	264.0

ES = electrospun; PCL = polycaprolactone; P3HB = poly(3-hydroxybutyrate); SF = silk fibroin.

crystalline nature (41), which was maintained even after the electrospinning process. For ES-P3HB (Tab. IV), 2 endothermic peaks were detected, the first one centered at 176.5°C, with an enthalpy value in the usual range of P3HB crystallinity (49). The second one, with a high enthalpy value (ΔH=512.6 J/g), was detected at 281°C, denoting a better organized crystalline structure compared with that of PCL. In fact, P3HB is a highly crystalline polyester with a high melting point, compared with the other biodegradable polyesters (49).

The DSC results obtained for the nano/micro hybrid structures (Tab. IV) prepared by coating SF yarns with ES-PCL or ES-P3HB and twisting showed, as expected, no substantial differences in the melting temperature and enthalpy values compared with the SF yarns. Thus the crystallinity of the SF twisted yarns was not influenced by the electrospinning procedure or by the presence of the electrospun polymers. The melting transitions of PCL or P3HB were not detectable in the thermograms of the hybrid structures, due to the low overall quantity of deposited nanofibers compared with that of the SF component, which does not allow for the identification of PCL or P3HB thermal transitions in the DSC traces.

FT-IR analyses

The FTIR spectra (ATR mode) of all samples are shown in Figures 6 and 7. Main infrared peak assignments are reported in Table V.

From the IR spectra analysis, it appears that in both nano/micro hybrid scaffolds, the SF structure was in a beta sheet conformation and that the ES-PCL or ES-P3HB coating did not interfere with the silk structure. The absence of shifts in the characteristic IR bands or the appearance of new peaks showed that there were no changes in the chemical structure of the silk substrate after the electrospinning process of PCL or P3HB.

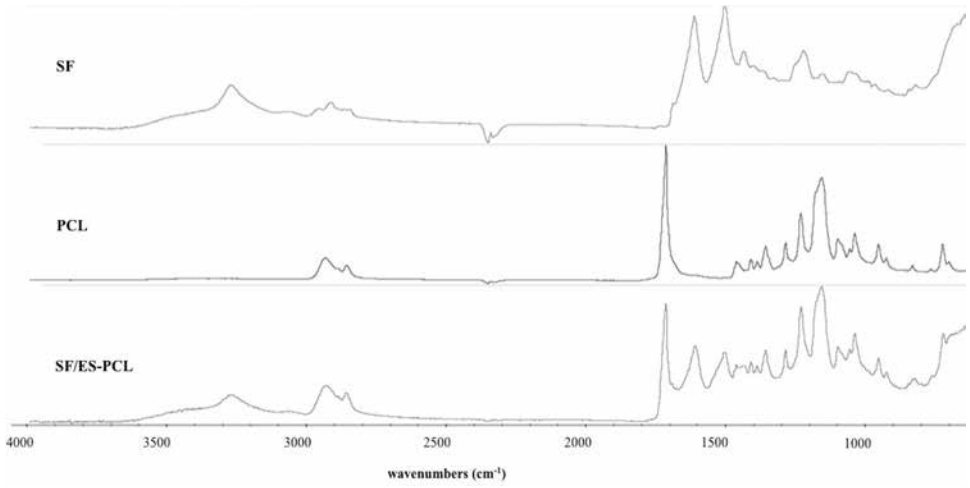

Fig. 6 - *Attenuated total reflectance–Fourier transform infrared (ATR-FTIR) spectra of SF, PCL nanofibers and SF/ES-PCL. ES = electrospun; PCL = polycaprolactone; SF = silk fibroin.*

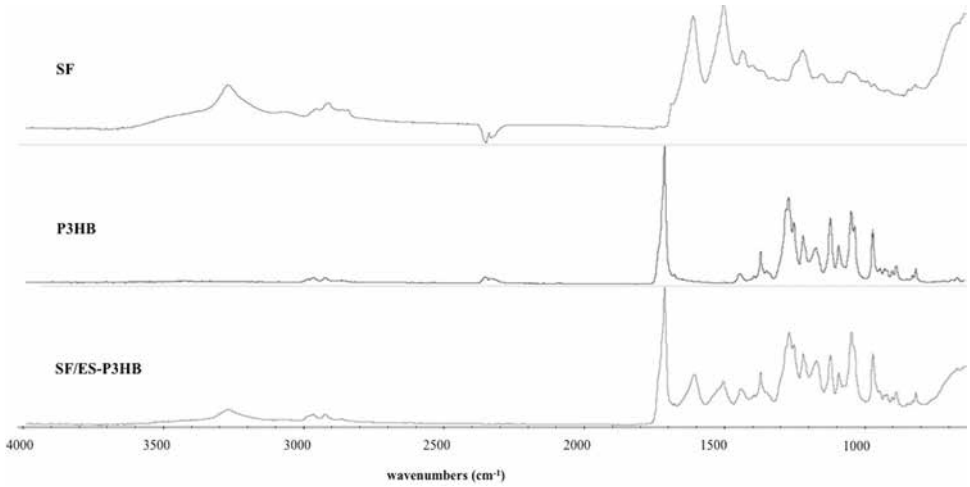

Fig. 7 - *Attenuated total reflectance–Fourier transform infrared (ATR-FTIR) spectra of SF, P3HB nanofibers and SF/ES-P3HB. ES = electrospun; P3HB = poly(3-hydroxybutyrate); SF = silk fibroin.*

TABLE V - INFRARED PEAK ASSIGNMENTS FOR SILK FIBROIN, PCL AND P3HB

Sample (ref.)	Wave numbers (cm^{-1})	Main assignments
Silk fibroin (50-52)	3,279	N-H stretching
	2,922	C-H stretching
	1,618	Amide I (C=O stretching)
	1,513	Amide II (C-N stretching + N-H in-plane bending)
	1,230	Amide III
PCL nanofibers (53, 54)	2,943-2,865	CH_2 stretching
	1,722	C=O stretching
	1,293	C-O and C-C stretching (crystalline phase)
	1,239-1,164	C-O-C stretching
P3HB nanofibers (55)	2,975	CH_3 stretching
	2,934	CH_2 stretching
	1,723	C=O stretching (crystalline)
	1,300-1,230	C-O-C stretching

PCL = polycaprolactone; P3HB = poly(3-hydroxybutyrate).

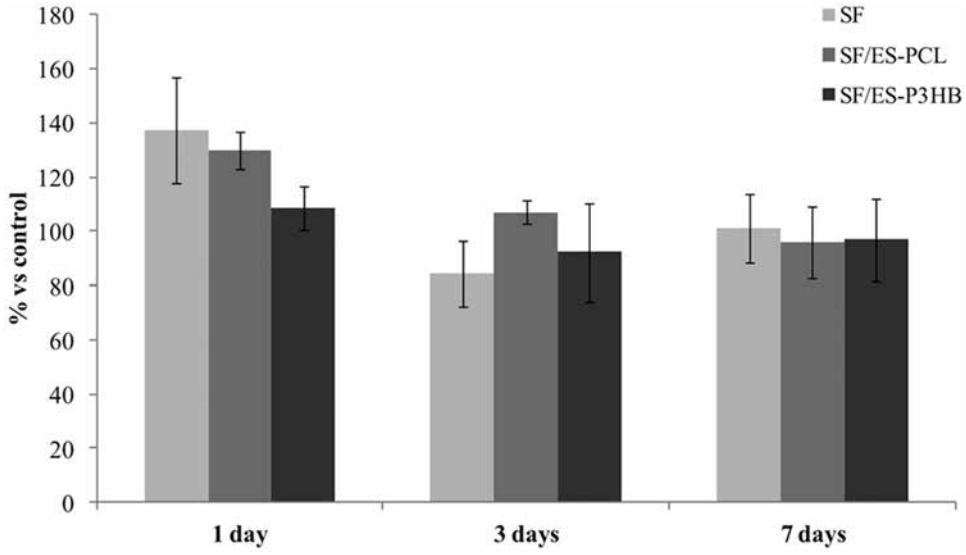

Fig. 8 - *Results of cytotoxicity assay. L929 cells were cultured in the presence of complete DMEM culture medium conditioned with SF, SF/ES-PCL and SF/ES-PH3B samples for 1, 3 and 7 days. After seeding, cell viability was determined by MTT assay. Results are expressed as means ± SD percentage of cells vs. control (cells cultured in the absence of sample extracts), of 3 independent experiments. ES = electrospun; PCL = polycaprolactone; P3HB = poly(3-hydroxybutyrate); SF = silk fibroin.*

In vitro cell interaction

L929 fibroblasts were cultured for 24 hours in the presence of the extracts obtained by conditioning the twisted structures of SF, SF/ES-PCL and SF/ES-P3HB in complete DMEM culture medium for 1, 3 and 7 days.

The results of the MTT assay for L929 viability are reported in Figure 8. The cells cultured in the presence of the extracts did not show any decrease in cell viability, and data were comparable with the control at each time point, with no significant differences among the 3 structures considered ($P>0.05$). Therefore, no cytotoxicity was observed for the prepared SF-based scaffolds in these test conditions.

By observing the L929 fibroblast proliferation at day 1, it can be seen that the values of cell viability shown in Figure 8 exceed 100% (i.e., are higher than the control, assumed = 100%). This can be explained by the possible release of short polypeptide sequences from SF yarns. In fact, SF is a protein mainly composed of amino acids such as alanine, glycine and serine, which are known to positively influence cell proliferation and metabolism (22).

Viability of L929 cells cultured in direct contact with SF, SF/ES-PCL and SF/ES-P3HB structures was evaluated in a preliminary test at 1 and 3 days after seeding (Fig. 9).

At 1 day of culture, the 3 structures showed high levels of cell viability, again with values exceeding the ones of the control (assumed as 100%), with no significant differences among them ($P>0.05$). Due to a technical problem which arose on day 2 of culture, the experiment ended at day 3. In fact, cell viability clearly decreased from the first to the third day after seeding, but the 2 hybrid structures showed a higher cell viability that the SF one, with a significant difference between SF and SF/ES-P3HB ($P<0.05$) and no significant differences between each other (SF/ES-PCL vs. SF/ES-PH3B).

In conclusion, the prepared nano/micro hybrid structures appear to be a promising substrate for L929 cell adhesion and proliferation. The combination of ES-PCL or ES-P3HB with SF yarns in the twisted nano/micro structure may constitute a good scaffold to promote and support cell growth up to the regeneration of ligamentous tissue or tendon. In vitro tests at longer time points should be carried out to investigate the influence of ES-P3HB or ES-PCL nanofibers on cell proliferation and colonization, suggestive of how the morphology of the underlying scaffold may affect ECM production.

CONCLUSIONS

This study represents the first investigation of the fabrication of nano/micro hybrid scaffolds composed of twisted SF yarns coated with PCL or P3HB electrospun nanofibers, in comparison with a scaffold made only of twisted SF yarns. The results obtained showed a slight enhancement of the tensile mechanical behavior, clearly due to an increase of internal forces derived from a positive interaction between nano and micro components.

Considering the effect of the electrospun nanofibers on the in vitro cell/material interaction, our results suggest that the novel nano/micro hybrid structures are able to encourage an appropriate in vitro behavior of fibroblastic cells in terms of adhesion, attachment and proliferation. Further investigations will allow for a better understanding of the interactions between the cells and the proposed scaffolds.

It is also worth noting that the mechanical properties of the hybrid structure can be tailored by changing

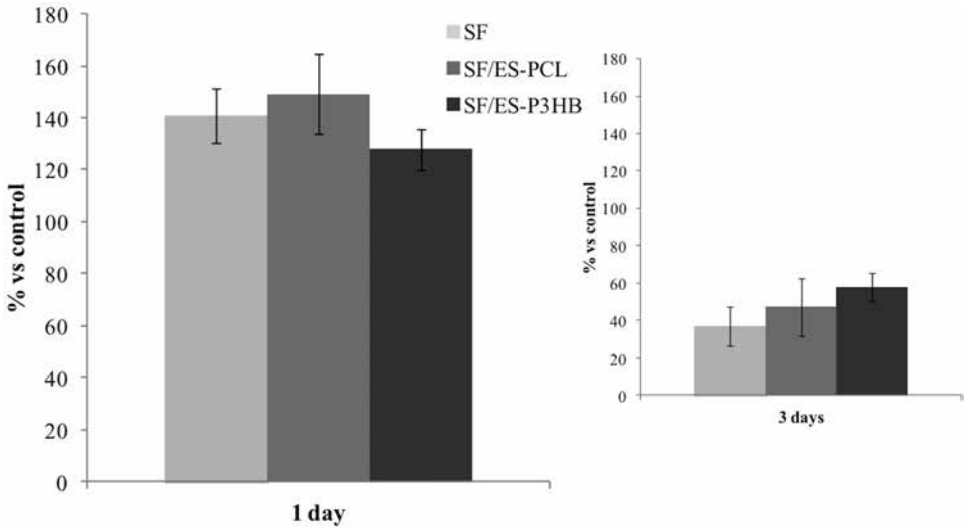

Fig. 9 - *Results of cytocompatibility assay. L929 cells were cultured in the presence of SF, SF/ES-PCL and SF/ES-PH3B samples for 1 and 3 days. L929 cell viability was determined by MTT assay. Results are expressed as means ± SD percentage of cells vs. control, of 3 independent experiments. ES = electrospun; PCL = polycaprolactone; P3HB = poly(3-hydroxybutyrate); SF = silk fibroin.*

the number of twisted SF yarns in the hybrid structure, to adapt the scaffold performance to the regeneration of different natural tendons and ligaments.

ACKNOWLEDGEMENTS

The authors are very grateful to Tianan Biologic Materials Co., Ltd (Ningbo, China) for providing poly (3-hydroxybutyrate, P3HB) and to Dr. G. Freddi and Dr. I. Donelli (INNOVHUB - SSI, Div. Stazione Sperimentale per la Seta, Milan, Italy) for their kind support in DSC and ATR-FTIR analysis. The individuals gave their contribution to the article and they gave their permission to have their names used in this manuscript.

Financial support: None.

Conflict of interest: None of the authors has any conflict of interest.

Address for correspondence:
Silvia Farè
Dipartimento di Chimica
Materiali e Ingegneria Chimica "G. Natta"
Politecnico di Milano
Piazza Leonardo da Vinci 32
IT-20133 Milan, Italy
silvia.fare@polimi.it

REFERENCES

1. Vieira AC, Guedes RM, Marques AT. Development of ligament tissue biodegradable devices: a review. J Biomech. 2009; 42(15): 2421-2430.
2. Sahoo S, Toh SL, Goh JC. PLGA nanofiber-coated silk microfibrous scaffold for connective tissue engineering. J Biomed Mater Res B Appl Biomater. 2010; 95(1): 19-28.
3. Kim HS, Seon JK, Jo AR. Current trends in anterior cruciate ligament reconstruction. current trends in anterior cruciate ligament reconstruction. Knee Surg Relat Res. 2013; 25(4): 165-173.
4. Leong NL, Petrigliano FA, McAllister DR. Current tissue engineering strategies in anterior cruciate ligament reconstruction. J Biomed Mater Res A. 2013.
5. Kumar K, Maffulli N. The ligament augmentation device: an historical perspective. Arthroscopy. 1999; 15(4): 422-432.
6. Legnani C, Ventura A, Terzaghi C, Borgo E, Albisetti W. Anterior cruciate ligament reconstruction with synthetic grafts: a review of literature. Int Orthop. 2010; 34(4): 465-471.
7. Petrigliano FA, McAllister DR, Wu BM. Tissue engineering for anterior cruciate ligament reconstruction: a review of current strategies. Arthroscopy. 2006; 22(4): 441-451.
8. Guidoin MF, Marois Y, Bejui J, Poddevin N, King MW, Guidoin R. Analysis of retrieved polymer fiber based replacements for the ACL. Biomaterials. 2000; 21(23): 2461-2474.
9. Ge Z, Yang F, Goh JC, Ramakrishna S, Lee EH. Biomaterials and scaffolds for ligament tissue engineering. J Biomed Mater Res A. 2006; 77(3): 639-652.
10. Ouyang HW, Goh JC, Thambyah A, Teoh SH, Lee EH. Knitted poly-lactide-co-glycolide scaffold loaded with bone marrow stromal cells in repair and regeneration of rabbit Achilles tendon. Tissue Eng. 2003; 9(3): 431-439.

11. Doroski DM, Brink KS, Temenoff JS. Techniques for biological characterization of tissue-engineered tendon and ligament. Biomaterials. 2007; 28(2): 187-202.
12. Kuo CK, Marturano JE, Tuan RS. Novel strategies in tendon and ligament tissue engineering: Advanced biomaterials and regeneration motifs. Sports Med Arthrosc Rehabil Ther Technol. 2010; 2: 20.
13. Dunn MG, Liesch JB, Tiku ML, Zawadsky JP. Development of fibroblast-seeded ligament analogs for ACL reconstruction. J Biomed Mater Res. 1995; 29(11): 1363-1371.
14. Lin VS, Lee MC, O'Neal S, McKean J, Sung KL. Ligament tissue engineering using synthetic biodegradable fiber scaffolds. Tissue Eng. 1999; 5(5): 443-452.
15. Lu HH, Cooper JA Jr, Manuel S, et al. Anterior cruciate ligament regeneration using braided biodegradable scaffolds: in vitro optimization studies. Biomaterials. 2005; 26(23): 4805-4816.
16. Tovar N, Murthy NS, Kohn J, Gatt C, Dunn M. ACL reconstruction using a novel hybrid scaffold composed of polyarylate fibers and collagen fibers. J Biomed Mater Res A. 2012; 100(11): 2913-2920.
17. Cristino S, Grassi F, Toneguzzi S, et al. Analysis of mesenchymal stem cells grown on a three-dimensional HYAFF 11-based prototype ligament scaffold. J Biomed Mater Res A. 2005; 73(3): 275-283.
18. Hansson A, Hashom N, Falson F, Rousselle P, Jordan O, Borchard G. In vitro evaluation of an RGD-functionalized chitosan derivative for enhanced cell adhesion. Carbohydr Polym. 2012; 90(4): 1494-1500.
19. Majima T, Irie T, Sawaguchi N, et al. Chitosan-based hyaluronan hybrid polymer fibre scaffold for ligament and tendon tissue engineering. Proc Inst Mech Eng H. 2007; 221(5): 537-546.
20. Chen J, Altman GH, Karageorgiou V, et al. Human bone marrow stromal cell and ligament fibroblast responses on RGD-modified silk fibers. J Biomed Mater Res A. 2003; 67(2): 559-570.
21. Fan H, Liu H, Toh SL, Goh JC. Anterior cruciate ligament regeneration using mesenchymal stem cells and silk scaffold in large animal model. Biomaterials. 2009; 30(28): 4967-4977.
22. Farè S, Torricelli P, Giavaresi G, et al. In vitro study on silk fibroin textile structure for anterior cruciate ligament regeneration. Mater Sci Eng C Mater Biol Appl. 2013; 33(7): 3601-3608.
23. Chen X, Qi YY, Wang LL, et al. Ligament regeneration using a knitted silk scaffold combined with collagen matrix. Biomaterials. 2008; 29(27): 3683-3692.
24. Fan H, Liu H, Wong EJ, Toh SL, Goh JC. In vivo study of anterior cruciate ligament regeneration using mesenchymal stem cells and silk scaffold. Biomaterials. 2008; 29(23): 3324-3337.
25. Altman GH, Diaz F, Jakuba C, et al. Silk-based biomaterials. Biomaterials. 2003; 24(3): 401-416.
26. Karamuk E, Mayer J, Raeber G. Tissue engineered composite of a woven fabric scaffold with tendon cells, response on mechanical simulation in vitro. Compos Sci. 2004; 64: 885-891.
27. Laurencin CT, Freeman JW. Ligament tissue engineering: an evolutionary materials science approach. Biomaterials. 2005; 26(36): 7530-7536.
28. Sahoo S, Cho-Hong JG, Siew-Lok T. Development of hybrid polymer scaffolds for potential applications in ligament and tendon tissue engineering. Biomed Mater. 2007; 2(3): 169-173.
29. Naghashzargara E, Semnania D, Karbasib S, Nekoeec H. Application of intelligent neural network method for prediction of mechanical behavior of wire-rope scaffold in tissue engineering. J Text I. 2014; 105: 264-274.
30. Wang X, Han C, Hu X, et al. Applications of knitted mesh fabrication techniques to scaffolds for tissue engineering and regenerative medicine. J Mech Behav Biomed Mater. 2011; 4(7): 922-932.
31. Cooper JA, Lu HH, Ko FK, Freeman JW, Laurencin CT. Fiber-based tissue-engineered scaffold for ligament replacement: design considerations and in vitro evaluation. Biomaterials. 2005; 26(13): 1523-1532.
32. Franco B, Vincenzo V, Alessandro DV, Tonello C, Abatangelo G, Mazzoleni F. Tissue engineering approaches for the construction of a completely autologous tendon substitute. Indian J Plast Surg. 2008; 41(1): 38-46.
33. Yin Z, Chen X, Chen JL, et al. The regulation of tendon stem cell differentiation by the alignment of nanofibers. Biomaterials. 2010; 31(8): 2163-2175.
34. Li WJ, Laurencin CT, Caterson EJ, Tuan RS, Ko FK. Electrospun nanofibrous structure: a novel scaffold for tissue engineering. J Biomed Mater Res. 2002; 60(4): 613-621.
35. Ma Z, Kotaki M, Inai R, Ramakrishna S. Potential of nanofiber matrix as tissue-engineering scaffolds. Tissue Eng. 2005; 11(1-2): 101-109.
36. Masaeli E, Morshed M, Rasekhian P, et al. Does the tissue engineering architecture of poly(3-hydroxybutyrate) scaffold affects cell-material interactions? J Biomed Mater Res A. 2012; 100(7): 1907-1918.
37. Zhang S. Fabrication of novel biomaterials through molecular self-assembly. Nat Biotechnol. 2003; 21(10): 1171-1178.
38. Smith LA, Ma PX. Nano-fibrous scaffold for tissue engineering. Colloid Surface B. 2004; 39: 125-131.
39. Sahoo S, Ouyang H, Goh JCH, Tay TE, Toh SL. Characterization of a novel polymeric scaffold for potential application in tendon/ligament tissue engineering. Tissue Eng. 2006; 12(1): 91-99.
40. Wu CS. A comparison of the structure, thermal properties, and biodegradability of polycaprolactone/chitosan and acrylic acid grafted polycaprolactone/chitosan. Polymer (Guildf). 2005; 46(1): 147-155.
41. Wang Y, Rodriguez-Perez MA, Reis RL, Mano JF. Thermal and thermomechanical behaviour of polycaprolactone and starch/polycaprolactone blends for biomedical application. Macromol Mater Eng. 2005; 290(8): 792-801.

42. Cheng ST, Chen ZF, Chen GQ. The expression of cross-linked elastin by rabbit blood vessel smooth muscle cells cultured in polyhydroxyalkanoate scaffolds. Biomaterials. 2008; 29(31): 4187-4194.
43. Zhou FL, Gong RH, Porat I. Nano-coated hybrid yarns using electrospinning. Surf Coat Tech. 2010; 204(21-22): 3459-3463.
44. Yoshimoto H, Shin YM, Terai H, Vacanti JP. A biodegradable nanofiber scaffold by electrospinning and its potential for bone tissue engineering. Biomaterials. 2003; 24(12): 2077-2082.
45. Rathbone S, Furrer P, Lübben J, Zinn M, Cartmell S. Biocompatibility of polyhydroxyalkanoate as a potential material for ligament and tendon scaffold material. J Biomed Mater Res A. 2010; 93(4): 1391-1403.
46. Tehrani AH, Zadhoush A, Karbasi S, Khorasani SN. Experimental investigation of the governing parameters in the electrospinning of poly(3-hydroxybutyrate) scaffolds: structural characteristics of the pores. J Appl Polym Sci. 2010; 118(5): 2682-2689.
47. Teh TK, Toh SL, Goh JC. Optimization of the silk scaffold sericin removal process for retention of silk fibroin protein structure and mechanical properties. Biomed Mater. 2010; 5(3): 035008.
48. Freddi G, Pessina G, Tsukada M. Swelling and dissolution of silk fibroin (Bombyx mori) in N-methyl morpholine N-oxide. Int J Biol Macromol. 1999; 24(2-3): 251-263.
49. Chaijamrus S, Udpuay N. Production and characterization of polyhydroxybutyrate from molasses and corn steep liquor produced by bacillus megaterium ATCC 6748. Agricultural Engineering International: The CIGR Ejournal, 2008; 10 Manuscript FP 07 030.
50. Lu Q, Hu X, Wang X, et al. Water-insoluble silk films with silk I structure. Acta Biomater. 2010; 6(4): 1380-1387.
51. Lu Q, Zhang B, Li M, et al. Degradation mechanism and control of silk fibroin. Biomacromolecules. 2011; 12(4): 1080-1086.
52. Um IC, Kweon HY, Park YH, Hudson S. Structural characteristics and properties of the regenerated silk fibroin prepared from formic acid. Int J Biol Macromol. 2001; 29(2): 91-97.
53. Elzein T, Nasser-Eddine M, Delaite C, Bistac S, Dumas PJ. FTIR study of polycaprolactone chain organization at interfaces. J Colloid Interface Sci. 2004; 273(2): 381-387.
54. Elzubair A, Elias CN, Suarez JC, Lopes HP, Vieira MV. The physical characterization of a thermoplastic polymer for endodontic obturation. J Dent. 2006; 34(10): 784-789.
55. Padermshoke A, Katsumoto Y, Sato H, Ekgasit S, Noda I, Ozaki Y. Melting behavior of poly(3-hydroxybutyrate) investigated by two-dimensional infrared correlation spectroscopy. Spectrochim Acta A Mol Biomol Spectrosc. 2005; 61(4): 541-550.